A Finite Element Formulation for Steady Transonic Euler Equations

A. Ecer* and H. U. Akay†
Purdue University at Indianapolis, Indianapolis, Indiana

Solution of two-dimensional, steady, transonic Euler equations is considered. Based on a variational principle, the problem is formulated in terms of three new Clebsch-type variables (ϕ, α, β). After a finite element formulation, a set of nonlinear equations is obtained in terms of these variables. This new formulation allows the Euler equations to be expressed in a second-order form, eliminating the difficulties encountered in the solution of first-order equations. It also provides a unified procedure for isentropic (potential) and nonisentropic (Euler) equations. A relaxation technique is employed to obtain steady-state solutions. Numerical results for flows through a channel are presented to demonstrate the effectiveness and accuracy of the numerical scheme.

Introduction

THE numerical solution of inviscid gasdynamic equations has been of interest to several investigators during the last two decades.[1,2] These problems have been generally analyzed by numerically integrating the unsteady Euler equations even to obtain steady-state solutions. A related development during the last decade has been in the numerical solution of steady, irrotational transonic flows.[3,4] Rather than integrating the unsteady flow equations, relaxation schemes have been employed for the direct solution of these steady potential flow equations.

The main objective of the present investigation is to develop a relaxation scheme for the analysis of inviscid, rotational, transonic flow problems. In this paper, first the variational formulation of inviscid, compressible flows is presented. Following the treatment of Seliger and Whitham,[5] a new variational form is developed for an efficient computation of steady Euler equations. The primary variables are the three Clebsch-type variables (ϕ, α, β), rather than the generally used (ρ, u, v, S). The governing equations, expressed in terms of these new variables, are diagonally dominant and each variable can be integrated separately. In the case of isentropic flows, the formulation reduces to a single equation with one variable: conservation of mass with the velocity potential ϕ. In fact, the developed computational method becomes an extension of the previous potential flow solution scheme of the present authors[6,7] to the steady Euler equations. The boundary conditions can be applied conveniently as a direct result of this variational principle. In Ref. 8, it has been shown that a similar formulation involving Clebsch-type transformations can also be applied to incompressible, viscous flow problems. Finally, the implementation of the finite element method using this variational principle provides a general tool for solving problems with arbitrary geometries.

Variational Formulation of the Euler Equations

The equations of motion for inviscid flows in Lagrangian coordinates can be obtained directly from the Hamilton's variational principle. To formulate the equations in a fixed coordinate system, however, an Eulerian-type variational principle is required. The derivation of an Eulerian variational principle which is employed in the present finite element formulation is described below.

Eulerian Variational Principles

In the Eulerian description, the Eulerian velocity vector $\boldsymbol{u}(\boldsymbol{x},t)$ is introduced, and the flow parameters $\boldsymbol{u}$, ρ, p, S are all taken to be functions of the position $\boldsymbol{x}$ in space at time t, without considering which fluid particle currently occupies the position $\boldsymbol{x}$.

The equations of motion in the Eulerian system are,

$$\rho\left(\frac{\partial u_i}{\partial t}+u_j\frac{\partial u_i}{\partial x_j}\right)=-\frac{\partial p}{\partial x_i} \qquad (i=1,2,3) \tag{1}$$

The equation of state defines the pressure p as a function of the mass density ρ and the entropy S as,

$$p=p(\rho,S) \tag{2}$$

The above set of equations become complete when the conservation of mass and entropy (or energy) are introduced as additional constraints,

$$\frac{\partial \rho}{\partial t}+\frac{\partial(\rho u_j)}{\partial x_j}=0 \tag{3}$$

$$\frac{\partial(\rho S)}{\partial t}+\frac{\partial(\rho u_j S)}{\partial x_j}=0 \tag{4}$$

Herivel[9] has first attempted to construct a variational principle for the above system of equations by formulating a variational functional for Eqs. (1) and (2). He introduced Eqs. (3) and (4) as side constraints to the functional through the use of Lagrangian multipliers. However, as pointed out by Lin[10,11] the extremals of such a principle yield only a subset of Euler equations, and the system is not complete without constraints defining the position of particles. Thus, he introduced the conservation equations,

$$\frac{\partial(\rho\alpha_i)}{\partial t}+\frac{\partial(\rho u_j\alpha_i)}{\partial x_j}=0 \tag{5}$$

for the identity of particles as additional constraints to the Herivel's variational functional, where (α_1, α_2, α_3) define the position of a particle at time $t=0$, and $\boldsymbol{x}(\boldsymbol{\alpha},t)$ is the position of a particle at time t. This subject was later investigated by Seliger and Whitham[5] who presented a broader view to the problem.

Presented as Paper 82-0062 at the AIAA 20th Aerospace Sciences Meeting, Orlando, Fla., Jan. 11-14, 1982; submitted Jan. 21, 1982; revision received May 24, 1982.

*Professor, School of Engineering and Technology. Member AIAA.

†Associate Professor, School of Engineering and Technology. Member AIAA.

A direct approach for constructing a variational functional in the Eulerian form is to express a Lagrangian density in terms of Eulerian variables. To complete the formulation, conservation equations for the identity of particles are imposed as side constraints. The corresponding variational principle then can be stated as

$$\delta\int_t\int_\Omega\left\{\frac{1}{2}\rho u_i^2-\rho E(\rho,S)+\beta_i\left[\frac{\partial(\rho\alpha_i)}{\partial t}+\frac{\partial(\rho u_j\alpha_i)}{\partial x_j}\right]\right\}\mathrm{d}\Omega\mathrm{d}t=0 \tag{6}$$

where $E=p/[\rho(\gamma-1)]$ is the internal energy per unit mass and γ the ratio of specific heats. By using the Jacobian J of the transformation from $\boldsymbol{x}$ to $\boldsymbol{\alpha}$ space, and knowing the initial distributions of density and entropy, we determine the values of these quantities at any position $\boldsymbol{x}(\alpha,t)$ as

$$\rho=\rho_0(\boldsymbol{\alpha})/J \tag{7}$$

and

$$S=S_0(\boldsymbol{\alpha}) \tag{8}$$

In Eq. (6), the constraints on material coordinates α_i are placed through the Lagrange multipliers β_i to insure that the functional is evaluated solely for the fluid particles occupying the Eulerian space $\Omega(\boldsymbol{x})$. Substituting Eqs. (7) and (8) into Eq. (6), and integrating by parts, the functional becomes

$$\delta\int_t\int_\Omega\rho(\alpha_{mn})\left[E(\alpha_{mn},\alpha_m)+\alpha_i\frac{\partial\beta_i}{\partial t}+\frac{1}{2}u_i^2\right]\mathrm{d}\Omega\mathrm{d}t=0 \tag{9}$$

where

$$\alpha_{mn}=\partial\alpha_m/\partial x_n \tag{10}$$

The variations of Eq. (9), taken with respect to u_i, α_i, β_i, lead to

$$\delta u_i:\quad u_i=\alpha_j\frac{\partial\beta_j}{\partial x_i},\quad (i=1,2,3) \tag{11}$$

$$\delta\alpha_i:\quad \rho\frac{\mathrm{D}\beta_i}{\mathrm{D}t}=\frac{\partial}{\partial x_j}\left[\left(E+\alpha_k\frac{\partial\beta_k}{\partial t}+\frac{1}{2}u_k^2\right)\frac{\partial\rho}{\partial\alpha_{ij}}+\rho\frac{\partial E}{\partial\alpha_{ij}}\right]-\rho\frac{\partial E}{\partial\alpha_i} \tag{12}$$

$$\delta\beta_i:\quad \frac{\partial(\rho\alpha_i)}{\partial t}+\frac{\partial(\rho\alpha_i u_j)}{\partial x_j}=0 \tag{13}$$

where

$$\frac{\mathrm{D}}{\mathrm{D}t}=\frac{\partial}{\partial t}+u_i\frac{\partial}{\partial x_i}$$

With the help of Eqs. (7) and (8), it can be verified that Eqs. (11-13) are equivalent to the equations of motion.[5]

If the velocity representation in Eq. (11) is assumed a priori, then α_i and β_i become the only primary dependent variables of this formulation. Although the variational functional in Eq. (9) appears to be simple, the fact that time derivative of β_i appears implicitly in Eq. (12) is inconvenient. Moreover, the evaluation of the Jacobian in Eq. (7) is somewhat cumbersome.

An alternative to functional in Eq. (9) is to introduce the conservation of mass as a side constraint with ϕ as the additional Lagrangian multiplier. In this case, one of the constraint equations for material coordinates may be dropped and the following variational statement is obtained:

$$\delta\int_t\int_\Omega\left\{\frac{1}{2}\rho u_i^2-\rho E(\rho,\alpha_1,\alpha_2)+\phi\left[\frac{\partial\rho}{\partial t}+\frac{\partial(\rho u_j)}{\partial x_j}\right]+\beta_1\left[\frac{\partial(\rho\alpha_1)}{\partial t}+\frac{\partial(\rho u_j\alpha_1)}{\partial x_j}\right]+\beta_2\left[\frac{\partial(\rho\alpha_2)}{\partial t}+\frac{\partial(\rho u_j\alpha_2)}{\partial x_j}\right]\right\}\mathrm{d}\Omega\mathrm{d}t=0 \tag{14}$$

The variations with respect to u_i,ρ,ϕ,β_k, and α_k $(i=1,2,3;\ k=1,2)$, lead to

$$\delta u_i:\quad u_i=\frac{\partial\phi}{\partial x_i}+\alpha_1\frac{\partial\beta_1}{\partial x_i}+\alpha_2\frac{\partial\beta_2}{\partial x_i} \tag{15}$$

$$\delta\rho:\quad H=-\frac{\partial\phi}{\partial t}-\alpha_1\frac{\partial\beta_1}{\partial t}-\alpha_2\frac{\partial\beta_2}{\partial t}-\frac{1}{2}u_i^2 \tag{16a}$$

$$=\frac{1}{2}u_i^2-\frac{\mathrm{D}\phi}{\mathrm{D}t}-\alpha_1\frac{\mathrm{D}\beta_1}{\mathrm{D}t}-\alpha_2\frac{\mathrm{D}\beta_2}{\mathrm{D}t} \tag{16b}$$

$$\delta\phi:\quad \frac{\partial\rho}{\partial t}+\nabla\cdot(\rho\boldsymbol{u})=0 \tag{17}$$

$$\delta\beta_k:\quad \frac{\partial(\rho\alpha_k)}{\partial t}+\nabla\cdot(\rho\alpha_k\boldsymbol{u})=0 \tag{18}$$

$$\delta\alpha_k:\quad \rho\frac{\partial\beta_k}{\partial t}+\rho\boldsymbol{u}\cdot\nabla\beta_k=-\frac{p}{R}\frac{\partial S}{\partial\alpha_k} \tag{19}$$

where ∇ is the gradient operator and the dot denotes the scalar product of two vectors. The evaluation of $\partial S/\partial\alpha_k$ from Eq. (8) completes the above formulation. In Eqs. (16), H is the specific enthalpy defined as

$$H=E+p/\rho \tag{20}$$

and in Eq. (19) R is the gas constant. If Eqs. (15) and (16) are assumed a priori, the primary dependent variables of the variational functional in Eq. (14) becomes ϕ, β_k, and α_k $(k=1,2)$. Although only two out of three material coordinates are needed as the primary variables in this variational statement, the third coordinate is still required to determine the entropy from the initial distribution as follows:

$$S=S_0(\alpha_i),\quad (i=1,2,3) \tag{21}$$

The formulation is complete with only two material coordinates, for the cases in which the far-field flow conditions can be defined by these two coordinates, e.g., a flow in which all particles emanate from a steady state. Similarly in such two-dimensional flows, only one coordinate suffices. In transonic flows, although material coordinates α_i are continuous across the shock, there is a sudden change in the entropy. However, since the entropy is not a primary variable of this formulation, the entropy discontinuities can be handled conveniently.

If one proceeds further with this approach to include the entropy as a primary dependent variable by introducing the conservation of entropy as a side constraint, one more equation for material coordinates may be dropped and Herivel-Lin variational principle is obtained.[5] It can be shown that the integrands in Eqs. (6) and (14) are equivalent to pressure indicating that each is a special case of Bateman's principle,

$$\delta\int_t\int_\Omega p\mathrm{d}\Omega\mathrm{d}t=0 \tag{22}$$

Variational Formulation of Steady Transonic Flows

The main objective of the present investigation is to analyze steady, transonic flows. The variational principle in Eq. (14) proves to be more convenient for this purpose. Here, further details of implementing Eq. (14) to steady, two-dimensional transonic flows are presented.

When the flow is steady and adiabatic, the total enthalpy

$$H_0=H+\tfrac{1}{2}u_i^2 \tag{23}$$

is constant along a streamline[11] and, except across a shock, the entropy S is also constant along a streamline. The change

in entropy across the shock, however, can be determined from the shock-jump relations. Isoenergetic and isentropic flows become special cases of this problem where H_0 and S, respectively, become constant everywhere.

If a streamline is defined as the intersection of the $\alpha_1=c_1$ and $\alpha_2=c_2$ planes, then H_0 and S can be expressed as functions of α_1 and α_2 only,

$$H_0=H_0(\alpha_1,\alpha_2), \quad S=S_0(\alpha_1,\alpha_2) \tag{24}$$

Hence, without having to introduce the conservation of entropy as an additional constraint, both H_0 and S can be calculated as functions of α_1 and α_2.

In the case of two-dimensional flow, the problem is reduced by an order, and only one material coordinate is required. One can then write

$$H_0=H_0(\alpha_1) \text{ and } S=S_0(\alpha_1) \tag{25}$$

where $\alpha_1=c_1$ is a curvilinear material coordinate normal to the flow direction. This is an important advantage since in the original Herivel-Lin formulation both S and α_1 have to be kept as primary dependent variables even for the two-dimensional case.

Letting $\alpha=\alpha_1$ and $\beta=\beta_1$, the variational statement in Eq. (14) is simplified as

$$\delta\pi=\delta\int_t\int_\Omega\left\{\frac{1}{2}\rho u_i^2-\rho E+\phi\left[\frac{\partial\rho}{\partial t}+\nabla\cdot(\rho\boldsymbol{u})\right]+\beta\left[\frac{\partial}{\partial t}(\rho\alpha)+\nabla\cdot(\rho\alpha\boldsymbol{u})\right]\right\}\mathrm{d}\Omega\mathrm{d}t=0 \tag{26}$$

Integrating by parts and allowing for nonzero variations on the boundaries for generality, Eq. (26) becomes,

$$\delta\pi=\delta\left\{\int_t\int_\Omega\left[\frac{1}{2}\rho u_i^2-\rho E-\rho\frac{\mathrm{D}\phi}{\mathrm{D}t}-\rho\alpha\frac{\mathrm{D}\beta}{\mathrm{D}t}\right]\mathrm{d}\Omega\mathrm{d}t+\int_t\int_{\Gamma_2\phi}f_\phi\phi\mathrm{d}\Gamma\mathrm{d}t+\int_t\int_{\Gamma_2\beta}f_\beta\beta\mathrm{d}\Gamma\mathrm{d}t\right\}=0 \tag{27}$$

where $\Gamma_2\phi$ and $\Gamma_2\beta$, respectively, denote those portions of boundaries on which the flux-type quantities

$$f_\phi=\rho\boldsymbol{u}\cdot\boldsymbol{n} \tag{28}$$

and

$$f_\beta=\rho\alpha\boldsymbol{u}\cdot\boldsymbol{n} \tag{29}$$

are specified. In the above $\boldsymbol{n}$ denotes the unit outward normal vector on the boundary.

Using Eq. (16b), it can further be shown that Eq. (27) becomes

$$\delta\pi=\delta\left\{\int_t\int_\Omega(\rho H-\rho E)\mathrm{d}\Omega\mathrm{d}t+\int_t\int_{\Gamma_2\phi}f_\phi\phi\mathrm{d}\Gamma\mathrm{d}t+\int_t\int_{\Gamma_2\beta}f_\beta\beta\mathrm{d}\Gamma\mathrm{d}t\right\}=0 \tag{30}$$

From Eq. (20) one can obtain,

$$\rho H-\rho E=p \tag{31}$$

which is independent of time for steady flows. Moreover, since f_ϕ and f_β are time-independent quantities on the boundaries, the time integration in Eq. (30) drops out for arbitrary variations of ϕ and β. Equation (27) can therefore be expressed as,

$$\delta\pi=\delta\left[\int_\Omega p\mathrm{d}\Omega+\int_{\Gamma_2\phi}f_\phi\phi\mathrm{d}\Gamma+\int_{\Gamma_2\beta}f_\beta\beta\mathrm{d}\Gamma\right]=0 \tag{32}$$

which is the Bateman's variational principle for steady flows.

Finally, by writing the perfect gas relation

$$p=\kappa\rho^\gamma e^{(\gamma-1)S/R} \tag{33}$$

and using the relation for total enthalpy

$$H_0(\alpha)=H+\frac{1}{2}u_i^2=\frac{\gamma}{\gamma-1}\frac{p}{\rho}+\frac{1}{2}u_i^2 \tag{34}$$

the variational principle for steady flows becomes

$$\delta\pi(\phi,\alpha,\beta)=\delta\left[\int_\Omega c\left(H_0-\frac{1}{2}u_i^2\right)^\theta e^{-S/R}\mathrm{d}\Omega+\int_{\Gamma_2\phi}f_\phi\phi\mathrm{d}\Gamma+\int_{\Gamma_2\beta}f_\beta\beta\mathrm{d}\Gamma\right]=0 \tag{35}$$

where in Eqs. (33-35)

$$u_i=\frac{\partial\phi}{\partial x_i}+\alpha\frac{\partial\beta}{\partial x_i} \tag{36}$$

$$H_0(\alpha)=H+\frac{1}{2}u_i^2=-\frac{\partial\phi}{\partial t}-\alpha\frac{\partial\beta}{\partial t} \tag{37}$$

$$\theta=\gamma/(\gamma-1), \quad c=\kappa(\kappa\theta)^{-\theta}, \quad \kappa=\text{const} \tag{38}$$

Both $S_0(\alpha)$ and $H_0(\alpha)$ in the above can be determined from the given far-field conditions.

The governing equations from Eq. (35) are

$$\delta\phi: \quad \nabla\cdot(\rho\boldsymbol{u})=0 \tag{39}$$

$$\delta\alpha: \quad \rho\boldsymbol{u}\cdot\nabla\beta=\rho\frac{\partial H_0}{\partial\alpha}-\frac{p}{R}\frac{\partial S}{\partial\alpha} \tag{40}$$

$$\delta\beta: \quad \nabla\cdot(\rho\alpha\boldsymbol{u})=0 \tag{41}$$

with

$$f_\phi=\rho\boldsymbol{u}\cdot\boldsymbol{n} \text{ on } \Gamma_2\phi \tag{42}$$

$$f_\beta=\rho\alpha\boldsymbol{u}\cdot\boldsymbol{n} \text{ on } \Gamma_2\beta \tag{43}$$

Equation (37) indicates that in general ϕ and β are not time independent even in the steady case. However, this presents no difficulty in the formulation since the total enthalpy

$$H_0(\alpha)=-\frac{\partial\phi}{\partial t}-\alpha\frac{\partial\beta}{\partial t} \tag{44}$$

for the steady state is constant along a streamline. Using Eq. (44), Eq. (40) becomes

$$\rho\frac{\partial\beta}{\partial t}+\rho\boldsymbol{u}\cdot\nabla\beta=-\frac{p}{R}\frac{\partial S}{\partial\alpha} \tag{45}$$

When the flow is isoenergetic H_0 is constant everywhere and, from Eq. (44), β becomes independent of time although ϕ is still dependent. For steady flows in which all particles emanate from a uniform state, the total energy H_0 and the entropy S_0 will be constant everywhere. The motion in general will be isentropic, isoenergetic, and irrotational until shock waves interfere. After the shock, the flow will remain isoenergetic, although no longer isentropic and irrotational. The entropy distribution after the shock, however, can be determined as a function of α using the Rankine-Hugoniot shock-jump conditions. Consequently, the entropy increase S_2-S_1 across the shock is simply calculated from the following expression:

$$S_2-S_1=\frac{R}{(\gamma-1)}\log_e\left[1+\frac{2\gamma}{\gamma+1}(M_{1n}^2-1)\right]-\gamma R\log_e\frac{(\gamma+1)M_{1n}^2}{(\gamma-1)M_{1n}^2+2} \tag{46}$$

where M_{1n} is the normal component of the upstream Mach number at the shock. Since the entropy distribution prior to shock is known, this allows the determination of entropy distribution

$$S=\bar{S}_0(\alpha) \tag{47}$$

past the shock.

The representation of the velocity field in the form

$$u=\nabla\phi+\alpha\nabla\beta \tag{48}$$

is known as the Clebsch[12] representation. The vorticity in this representation is given by

$$\zeta=\nabla\times u=\nabla\alpha\times\nabla\beta \tag{49}$$

For the special case of isoenergetic and isentropic flows the vorticity vanishes, since from Eq. (40),

$$u\cdot\nabla\beta=0 \tag{50}$$

Also, from Eqs. (40) and (48) the velocity representation simply takes the familiar form

$$u=\nabla\phi \tag{51}$$

Finite Element Formulation of Euler Equations

Governing Equations and Boundary Conditions

Equations (39-41) are employed for the finite element formulation of the steady Euler equations. These new sets of equations satisfy all conservation laws and are obtained directly from a variational principle. For two-dimensional isoenergetic flows, using the Clebsch representation in Eq. (48), Eqs. (39-41) can be rearranged as follows:

$$\nabla\cdot(\rho\nabla\phi)+\nabla\cdot(\rho\alpha\nabla\beta)=0 \tag{52}$$

$$(1/T)u\cdot\nabla\beta=-S_{,\alpha} \tag{53}$$

$$\nabla\cdot(\rho\alpha u)=0 \tag{54}$$

with the flux-type boundary conditions

$$\rho u\cdot n=f_\phi \text{ on } \Gamma_2\phi \tag{55}$$

$$\rho\alpha u\cdot n=f_\beta \text{ on } \Gamma_2\beta \tag{56}$$

and the forced-type boundary conditions

$$\phi=\phi_0 \text{ on } \Gamma_1\phi \tag{57}$$

$$\beta=\beta_0 \text{ on } \Gamma_1\beta \tag{58}$$

$$\alpha=\alpha_0 \text{ on } \Gamma_1\alpha \tag{59}$$

where in Eq. (53), T denotes temperature and $S_{,\alpha}=\partial S/\partial\alpha$. It was shown through the variational formulation that no flux-type boundary conditions are required for the variable α.

As can be seen from these equations, while Eq. (52) is a second-order equation, Eqs. (53) and (54) basically describe the convection of the variables α and β. The above formulation of the Euler equations in terms of the basic variables ϕ, α, and β has certain advantages when compared with the more standard form of Euler equations expressed with ρ, u, v, and S as the primary variables. One of the basic difficulties in the solution of Euler equations related to the propagation of waves in subsonic regions[13] is treated in the present formulation by restricting the convective behavior of the vorticities only in Eqs. (53) and (54), while Eq. (52) is still elliptic.

The numerical solution of Eq. (52) is attempted in the present study based on the experience obtained from the solution of transonic potential flows. The additional development of the computational procedure involves basically the solution of Eqs. (53) and (54). At first, these equations were considered consisting of purely convective, first-order differential operators. Numerical solutions were obtained by introducing small artificial viscosity terms (upwinding) and by numerically integrating these equations. After some experimentation with these schemes, the accuracy of the obtained numerical solutions was found to be unsatisfactory. Thus, for the solution of these convection equations, the following new procedure is proposed: Eqs. (53) and (54) are cast into the form of two second-order equations, by applying the convection operator once more as,

$$\rho u\cdot\nabla\left(\frac{1}{T}u\cdot\nabla\beta\right)=0 \tag{60}$$

$$\rho u\cdot\nabla(\rho u\cdot\nabla\alpha)=0 \tag{61}$$

with the flux-type boundary conditions

$$f_\beta=0 \text{ on } \Gamma_2\beta \tag{62}$$

$$-S_{,\alpha}(\rho u\cdot n)=f_\alpha \text{ on } \Gamma_2\alpha \tag{63}$$

The right-hand side of Eq. (60) vanishes since the entropy is constant along a streamline. Conservation of mass [Eq. (52)] is utilized in obtaining Eq. (61). It can be shown that Eq. (53) in fact corresponds to Crocco's equation for vorticity transport. Equation (61) provides the streamlines for a given velocity field, which in turn provides the vorticity distribution everywhere.

The boundary conditions for this new set of equations are interesting. At a boundary, they require either a forced-type boundary condition (specification of ϕ, α, and β) or a flux-type boundary condition which is a natural boundary condition. This provides a very useful tool for specifying the boundary conditions. For example, at the inlet boundary, ϕ, α, and β are specified for each streamline. At the exit, a flux-type boundary condition for the conservation of mass is specified using Eq. (55). For the material coordinate α, the flux-type boundary condition is homogeneous as can be seen in Eq. (62). Equation (63) specifies the flux-type boundary condition for the conservation of β. In this case, $S_{,\alpha}$ is calculated from the entropy distribution across the shock using Eqs. (46) and (47). On solid boundaries all flux terms vanish.

Galerkin Formulation and Finite Element Approximation

For the Galerkin formulation of the problem, Eqs. (52), (60), and (61) are expressed in a weak form as follows:

$$\delta\pi=\int_\Omega\left[\rho\nabla\phi\cdot\nabla\delta\phi+\rho\alpha\nabla\beta\cdot\nabla\delta\phi+\frac{1}{T}(u\cdot\nabla\beta)(\rho u\cdot\nabla\delta\alpha)\right.$$
$$\left.+(\rho u\cdot\nabla\alpha)(\rho u\cdot\nabla\delta\beta)\right]d\Omega-\int_{\Gamma_2\phi}f_\phi\delta\phi d\Gamma$$
$$-\int_{\Gamma_2\alpha}f_\alpha\delta\alpha d\Gamma=0 \tag{64}$$

where the flux f_ϕ is as defined in Eq. (55), and f_α is as defined in Eq. (63).

Bilinear shape functions $N_i(x,y)$ are chosen for each dependent variable, and for a four-noded element e, the following approximations are made:

$$\phi(x,y)=N_i(x,y)\phi_i^e=N^T\phi^e, \quad (i=1,\ldots,4) \tag{65}$$

$$\alpha(x,y)=N_i(x,y)\alpha_i^e=N^T\alpha^e \tag{66}$$

$$\beta(x,y)=N_i(x,y)\beta_i^e=N^T\beta^e \tag{67}$$

where ϕ_i^e, α_i^e, and β_i^e are the nodal point values of the dependent variables ϕ, α, and β, respectively.

By expressing the functional in Eq. (64) for an element e, substituting Eqs. (65-67) into Eq. (64), and repeating this procedure for all elements, the following system of coupled equations are obtained:

$$K_{\phi\phi}\phi + K_{\phi\beta}\beta = f_\phi \tag{68}$$

$$K_{\alpha\beta}\beta = f_\alpha \tag{69}$$

$$K_{\beta\alpha}\alpha = 0 \tag{70}$$

where

$$K_{\phi\phi} = \sum_e \int_{\Omega_e} \rho (N_{,x} N_x^T + N_{,y} N_y^T)\, d\Omega \tag{71}$$

$$K_{\phi\beta} = \sum_e \int_{\Omega_e} \rho\alpha (N_{,x} N_x^T + N_{,y} N_y^T)\, d\Omega \tag{72}$$

$$K_{\alpha\beta} = \sum_e \int_{\Omega_e} \frac{\rho}{T} (uN_{,x} + vN_{,y})(uN_x^T + vN_y^T)\, d\Omega \tag{73}$$

$$K_{\beta\alpha} = \sum_e \int_{\Omega_e} (\rho u N_{,x} + \rho v N_{,y})(\rho u N_x^T + \rho v N_y^T)\, d\Omega \tag{74}$$

$$f_\phi = \sum_e \int_{\Gamma_{2\phi}} (\rho u \cdot n) N\, d\Gamma \tag{75}$$

$$f_\alpha = -\sum_e \int_{\Gamma_{2\alpha}} S_{,\alpha} (\rho u \cdot n) N\, d\Gamma \tag{76}$$

and u and v are components of local velocity in x and y directions, respectively.

Solution of the Equations

To obtain the solution of the steady-state equations shown in Eqs. (68-70), a pseudo-time integration of these equations is considered,

$$K_{\phi\phi}^n \bar{\phi}^{n+1} = f_\phi^n - K_{\phi\beta}^n \bar{\beta}^{n+1} \tag{77}$$

$$K_{\alpha\beta}^n \bar{\beta}^{n+1} = f_\alpha^n \tag{78}$$

$$K_{\beta\alpha}^n \bar{\alpha}^{n+1} = 0 \tag{79}$$

with

$$\phi^{n+1} = (1-\omega)\phi^n + \omega\bar{\phi}^{n+1}, \text{ etc.} \tag{80}$$

where ω is a relaxation factor. As can be seen from Eqs. (77) and (78), the boundary fluxes are calculated from the values of ρ, u, and $S_{,\alpha}$ at the previous time step. The density is upwinded for all supersonic elements.[6]

The formulation of Euler equations in the form given by Eqs. (77-79) is computationally quite efficient. Equation (77) provides the solution for the irrotational flow by itself since β becomes a constant. For rotational flows, ϕ is calculated for each (α,β) distribution at each iteration step until the solution converges. The formulation is general in detecting isentropic regions of the flow during the iterations. Euler equations can be solved only for the nonisentropic flow regions for better efficiency. $K_{\phi\phi}$ is same as the coefficient matrix employed for solution of isentropic, transonic flows. $K_{\alpha\beta}$ and $K_{\beta\alpha}$ are the coefficient matrices for determining the convection of α and β terms. All three matrices are symmetric and positive definite.

Discussion of Numerical Results and Conclusions

Transonic flow through a parallel channel with a 4.2% thick circular-arc bump and an upstream Mach number of 0.85 is considered to test the developed computational scheme. Numerical solutions to this problem have been reported by several researchers at the 1979 GAMM workshop.[14] The sheared Cartesian grid with 44×8 elements shown in Fig. 1 was employed for the present analysis.

Assuming the flow to be isentropic and irrotational, the problem was first analyzed by solving the conservation of mass equation only. The computed isentropic pressure distribution over the circular bump is compared in Fig. 2 with the two representative solutions in the GAMM workshop. Mach contours of this case obtained with the present algorithm are as given in Fig. 3. It may be observed that the flow is close to choke. For the same problem Veuillot[14] predicts choke, whereas the remaining GAMM workshop solutions have not reached choke conditions. Since the GAMM workshop grid was considerably finer than the one shown in Fig. 1, the irrotational problem was analyzed once more using a refined grid with 60×12 elements. The results of the two grids are in good agreement as shown in Fig. 4.

The solution of the Euler equations, which takes into account the entropy changes at the shock, alters the pressure distribution only slightly, as can be observed in Fig. 5. Shown in Fig. 6 is the further comparison of pressures with the Euler solutions of Veuillot and Zannetti.[14] As can be observed, these solutions compare favorably within discretization accuracy. The obtained contours for the Mach numbers and the material coordinate α are respectively given in Figs. 7 and 8.

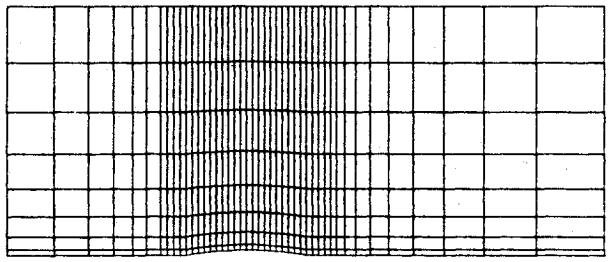

Fig. 1 Finite element grid (A, coarse).

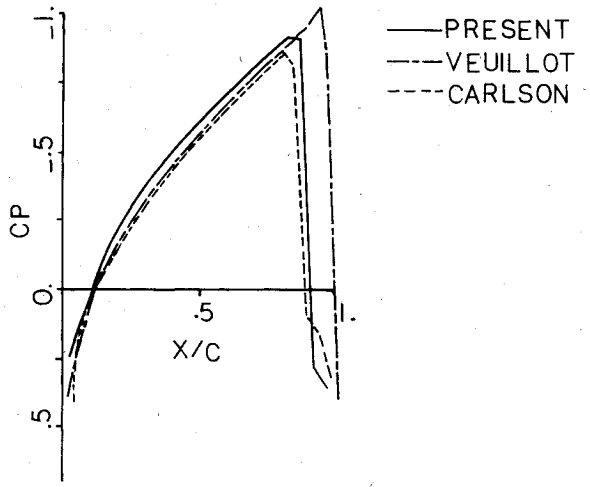

Fig. 2 Irrotational flow pressure distributions.

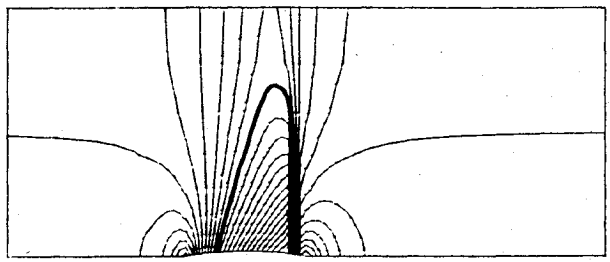

Fig. 3 Irrotational flow Mach contours (grid A, $\Delta M = 0.025$).

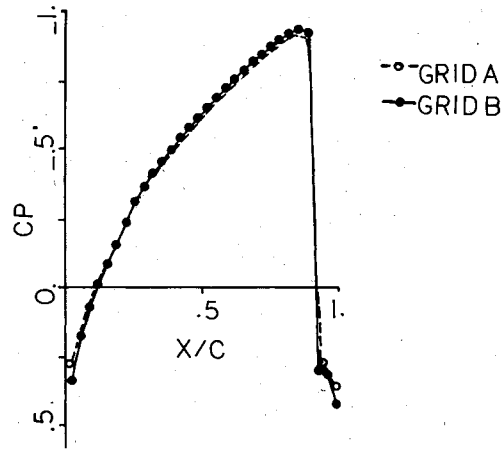

Fig. 4 Pressure distributions for two different grids.

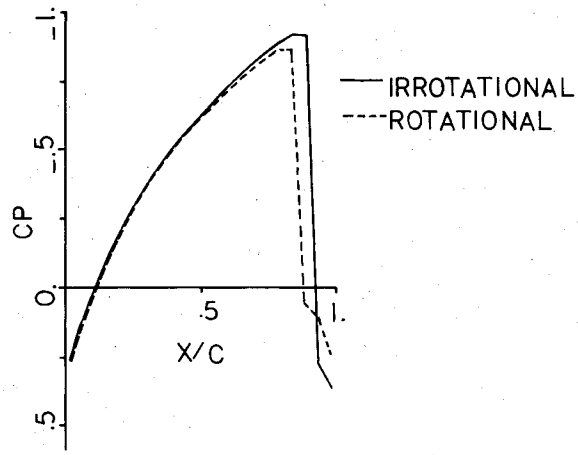

Fig. 5 Comparison of pressure distributions for rotational vs irrotational flows (grid A).

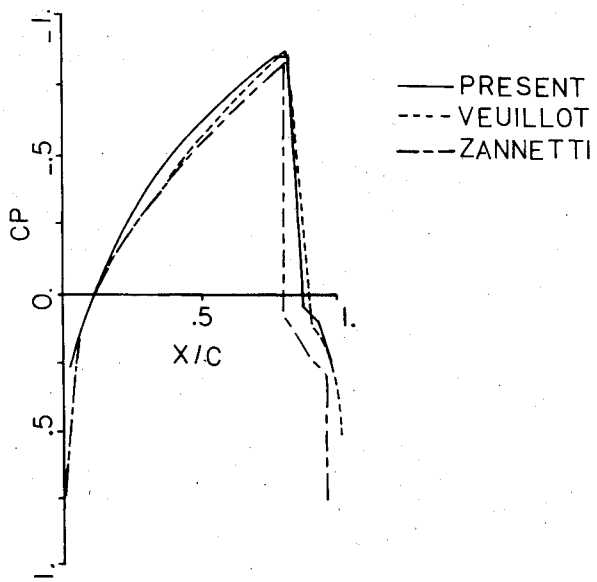

Fig. 6 Rotational flow pressure distributions.

The secondary variables in this formulation are ρ, q, p, and ζ which are derived by direct differentiation of the primary variables. Out of all secondary variables, the most sensitive quantity is the vorticity ζ. Hence, an assessment of the accuracy of the present scheme can be made by observing the convection of the vorticities through the channel. The vorticity can be calculated from Eq. (49) as

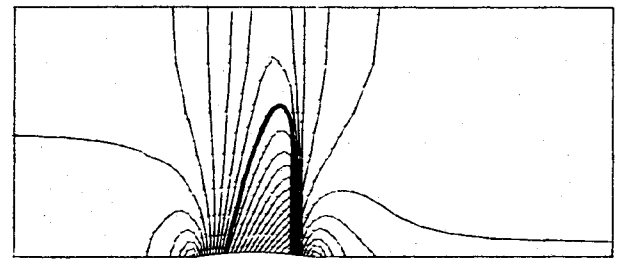

Fig. 7 Rotational flow Mach contours (grid A, $\Delta M = 0.025$).

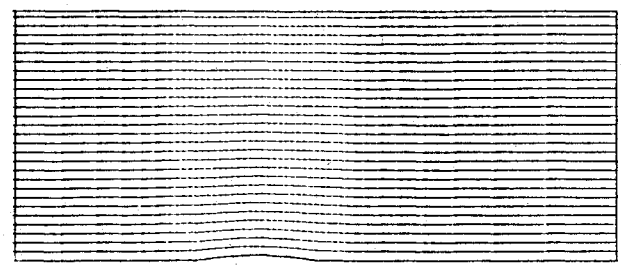

Fig. 8 Contours for material coordinate α ($\Delta\alpha = 0.075$, $\alpha_{min} = 0$, $\alpha_{max} = 2.073$).

$$\zeta = |\nabla\alpha \times \nabla\beta| = -\alpha_{,n}\beta_{,s} \tag{81}$$

where s is the flow direction and n the normal to s.

From Eqs. (53) and (81), the vorticity can also be computed using the following expression:

$$\zeta = \frac{p}{\rho q R} S_{,n} = \frac{T}{q} S_{,n} \tag{82}$$

where

$$q^2 = (u^2 + v^2) \tag{83}$$

Equation (82) is a special form of Crocco's theorem for two-dimensional flows.[11] Also, due to Crocco it is known that

$$\frac{\zeta}{p} = \frac{S_{,n}}{\rho q R} = \text{const} \tag{84}$$

on streamlines. Therefore, a good accuracy check is to observe if $\zeta/p = \text{const}$ lines follow the $\alpha = \text{const}$ lines. In addition, the two nondimensionalized vorticity values

$$\bar{\zeta} = \frac{\zeta C/a_0}{p/p_0} = -\frac{\alpha_{,n}\beta_{,s} C/a_0}{p/p_0} \tag{85}$$

and

$$\bar{\bar{\zeta}} = \frac{\zeta C/a_0}{p/p_0} = \frac{S_{,n} C/a_0}{\rho q R/p_0} \tag{86}$$

are computed for comparison, where C is the chord length of bump, a_0 the stagnation speed of sound, and p_0 the stagnation pressure. Contours for nondimensionalized vorticity/pressure values $\bar{\zeta}$ are shown in Fig. 9. As may be observed by comparing with Fig. 8, they match α contours very closely. Contours for $\bar{\bar{\zeta}}$ follow precisely the same trend hence not shown.

In Fig. 10 is shown the variation of the computed nondimensionalized vorticity/pressure values $\bar{\zeta}$ and $\bar{\bar{\zeta}}$ at different cross sections with respect to the material coordinate α. As can be seen from these results, the vorticity generated at the

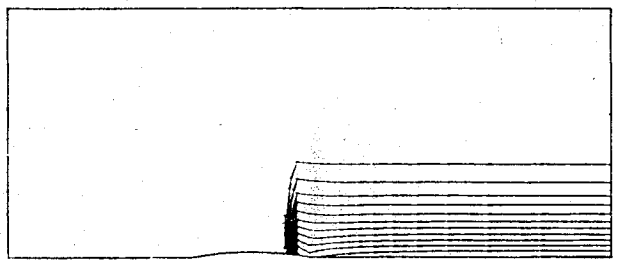

Fig. 9 Nondimensionalized velocity/pressure contours ($\Delta\bar{\zeta}=0.0075$).

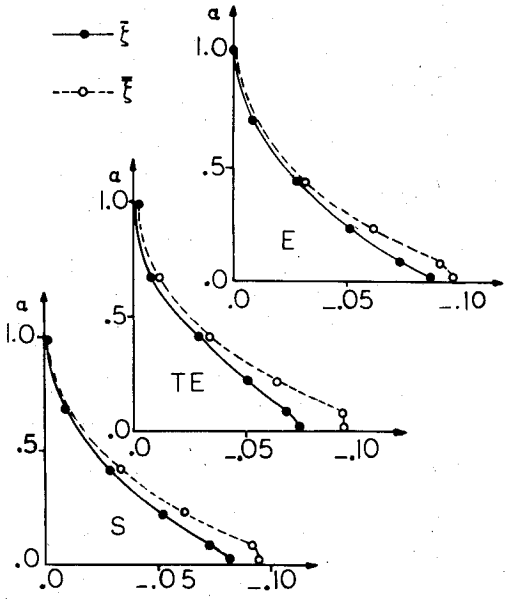

Fig. 10 Nondimensionalized vorticity/pressure profiles (S = immediately past the shock, TE = trailing edge, E = exit).

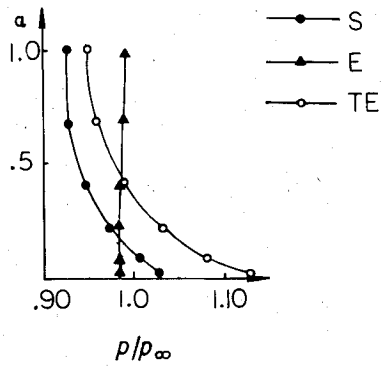

Fig. 11 Pressure vs α at different cross sections.

shock is convected to the downstream without any noticeable diffusion. The profiles at the immediate downstream of the shock and at the exit of the channel match almost identically. This is due to the formulation of the vorticity transport by two second-order equations rather than first-order convection equations. Since no artificial viscosity is needed, no artificial diffusion is observed. There is a slight perturbation at the trailing edge of the bump. This indicates that more refinement is needed in that region. However, it does not seem to affect the overall convection of the vorticity values throughout the rest of the channel. The perturbation is in fact due to the discretization errors in the calculation of pressure at the trailing edge rather than vorticities. Also, $\bar{\zeta}$ and $\bar{\bar{\zeta}}$ values deviate as they approach to the surface ($\alpha=0$) due to inadequate resolution. This is attributed primarily to the

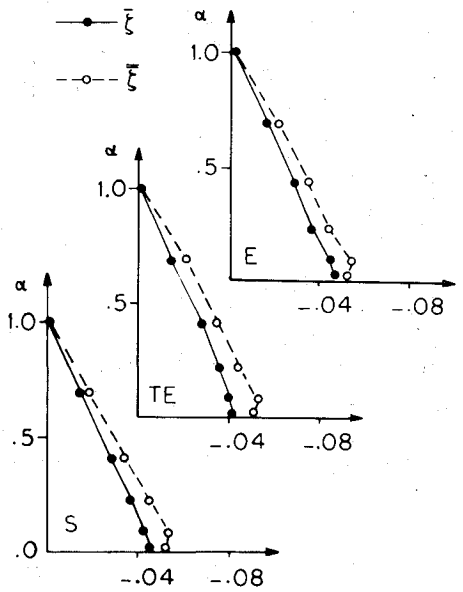

Fig. 12 Nondimensionalized vorticity/pressure profiles for quadratic assumption of $S=\bar{S}_0(\alpha)$.

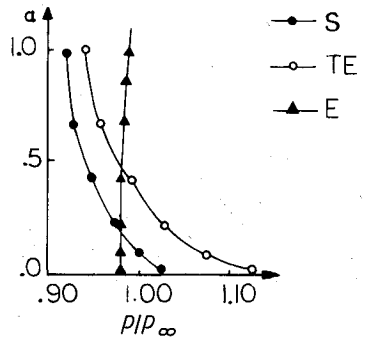

Fig. 13 Pressure vs α curves for quadratic assumption of $S=\bar{S}_0(\alpha)$.

coarseness of the grid in normal directions to the surface. However, deviations are still within acceptable limits. Nondimensionalized pressure profiles p/p_∞ at three cross sections shown in Fig. 11 indicate sharp gradients near the wall surfaces at both the trailing edge and immediately past the shock.

$S=\bar{S}_0(\alpha)$ distribution at the shock was obtained by using a cubic least-square fit for the calculated values of entropy change in each element along the shock. This allows a quadratic distribution of $S_{,\alpha}(\alpha)$ values across the cross sections. The near-quadratic variations of the computed vorticity values except near the solid wall boundaries indicate the accuracy of the solution. The use of a quadratic least-square fit for the $S=\bar{S}_0(\alpha)$ distributions changes the vorticity variation slightly while the other quantities remain virtually the same. The vorticity profiles for quadratic variations are shown in Fig. 12 and the pressure profiles are shown in Fig. 13.

The variations of the nonisentropic pressure correction factor

$$e^{(\gamma-1)S(\alpha)/R} \tag{87}$$

with respect to α are plotted in Fig. 14 for both quadratic and cubic distributions of $S=\bar{S}_0(\alpha)$. As can be observed, the differences between quadratic and cubic assumptions are small. Calculated exit angles for the nonisentropic solution were relatively small in this particular test case.

The same numerical results were obtained by starting the numerical integrations with either the uniform flow or the isentropic transonic flow solution as initial guesses. When the

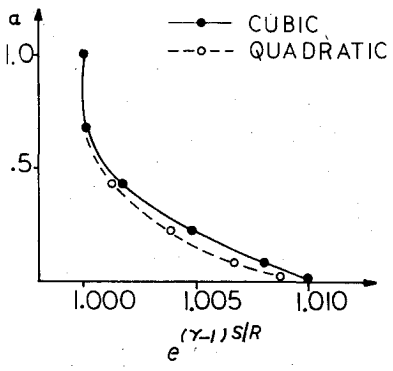

Fig. 14 Pressure correction factor vs α for quadratic and cubic assumptions of $S=S_0(\alpha)$.

uniform initial flow condition was used, a total of 610 iterations were needed for the final solution. When the isentropic transonic flow condition was used as an initial guess, however, a total of 400 iterations were needed, out of which 260 were used to obtain the isentropic solution first. In either case, an under-relaxation factor of $\omega=0.1$ was employed for all three variables ϕ, α, and β, which is a rather conservative value.

The presented numerical method describes the mathematical formulation and the application of a numerical method for the direct solution of steady Euler equations. The development of the procedure as an extension of existing potential flow formulations provides the applicability of the previous procedures, e.g., proper application of the artificial viscosity for supersonic elements, accurate modeling of the shock, etc.[6,7] On the other hand, the formulation of the vorticity transport in an elliptic form considerably reduces the difficulty of integrating the convection of inviscid, rotational flows. The convergence characteristics of the solution scheme and further numerical examples are currently being investigated.

Acknowledgments

This research was sponsored by NASA Lewis Research Center, Cleveland, Ohio, under Grant NSG-3294. The authors would like to thank R. V. Chima and P. M. Sockol for their valuable suggestions and encouragement. Computer services provided by the IUPUI Computer Center are gratefully acknowledged.

References

[1] Magnus, R. and Yoshihara, H., "Inviscid Transonic Flow Over Airfoils," AIAA Paper 70-47, 1970.

[2] Warming, R.F. and Beam, R. M., "Upwind Second-Order Difference Schemes and Applications in Aerodynamic Flows," *AIAA Journal*, Vol. 14, Sept. 1976, pp. 1241-1249.

[3] Murman, E. M. and Cole, J. D., "Calculation of Plane Steady Transonic Flows," *AIAA Journal*, Vol. 9, Jan. 1971, pp. 114-121.

[4] Jameson, A., "Iterative Solution of Transonic Flows Over Airfoils and Wings," *Communications in Pure and Applied Mathematics*, Vol. 2, No. 3, May 1974, pp. 283-309.

[5] Seliger, R. L. and Whitham, G. C., "Variational Principles in Continuum Mechanics," *Proceedings of Royal Society*, Vol. A 305, 1968, pp. 1-25.

[6] Ecer, A. and Akay, H. U., "Investigation of Transonic Flow in a Cascade Using the Finite Element Method," *AIAA Journal*, Vol. 19, Sept. 1981, pp. 1174-1182.

[7] Akay, H. U. and Ecer, A., "Finite Element Analysis of Transonic Flows in Highly Staggered Cascades," *AIAA Journal*, Vol. 20, March 1982, pp. 410-416.

[8] Ecer, A., "Variational Formulation of Viscous Flows," *International Journal of Numerical Methods in Engineering*, Vol. 15, Sept. 1980, pp. 1355-1361.

[9] Herivel, J. W., "The Derivation of the Equations of Motion of an Ideal Fluid by Hamilton's Principle," *Proceedings of the Cambridge Philosophical Society*, Vol. 51, 1955, pp. 344-349.

[10] Lin, C. C., "Hydrodynamics of Helium, II: Liquid Helium," *Proceedings of International School of Physics*, Course XXI, edited by G. Careri, Academic Press, New York, 1963, pp. 93-146.

[11] Serrin, J., "Mathematical Principles of Classical Fluid Mechanics," *Handbuch Der Physik*, Vol. VIII/I, edited by S. Flugge, Springer Verlag, Berlin, 1959, pp. 125-263.

[12] Clebsch, A., "Ueber Eine Allgemeine Transformation d. Hydrodynamischen Gleichungen," *Journal fuer die reine und angewandte Mathematik*, Vol. 56, 1859, pp. 1-10.

[13] Steger, J. L. and Warming, R. F., "Flux Vector Splitting of the Inviscid Gasdynamic Equations with Application to Finite-Difference Methods," *Journal of Computational Physics*, Vol. 40, No. 2, April 1981, pp. 263-293.

[14] *GAMM Workshop on Numerical Methods for the Computation of Inviscid Transonic Flow with Shock Waves*, The Aeronautical Research Institute of Sweden, Stockholm, Sept. 1979.